

Computational performance analysis of a two-slotted bucket Savonius rotor

CHASIOTIS VASILEIOS¹, TACHOS NIKOLAOS², FILIOS ANDRONIKOS¹

¹Department of Mechanical Engineering, University of West Attica, GR12244 Egaleo
GREECE

²Department of Materials Science and Engineering, University of Ioannina, GR45110 Ioannina
GREECE

Abstract: - The objective of the current computational study is to predict the performance output of a modified two-bucket Savonius rotor. Each bucket consists of three arc-type blades of different radius which is determined by the slot width ratio, in the range of 0.05 to 0.15 and the slot central angle, in the range of 0 to 20 deg. Nine configurations are designed with a fixed rotor diameter and a variable slot width and slot central angle, aiming to resolve the performance output and investigate the effect of the two previous parameters on the power and the static torque coefficients. The commercial CFD package Fluent[®] is used to solve the unsteady Reynolds-Averaged Navier-Stokes equations, along with Spalart-Allmaras turbulence model. Initially, a standard Savonius rotor, was used to validate the computational procedure using experimental results available in literature. Next, the same validated model is used to resolve the designed slotted bucket configurations. The performance of the examined slotted bucket configurations indicates improved self-starting characteristics, but a lower power coefficient compared with the solid bucket Savonius rotor. Lower values of slot width ratio have improved output performance while the slot central angle, does not greatly affect the overall performance of slotted bucket rotor.

Key-Words: - Vertical Axis Wind Turbines; Savonius rotor; Slotted bucket rotor; Computational Fluid Dynamics (CFD)

Received: May 12, 2021. Revised: January 20, 2022. Accepted: February 17, 2022. Published: March 24 2022.

Nomenclature

A_0	Wind turbine rotor swept area (m ²)	Re	Reynolds number per unit length, $Re = \rho_\infty V_\infty / \mu_\infty$
b	Radial interspace between two overlapping blades or slot width (m)	s	Length of the overlapping part of the blade or slot length (m)
c	Rotor gap distance (m)	T	Turbine rotor torque (N·m)
C_P	Power coefficient, $c_P = T\omega / (q_\infty V_\infty A_0)$	V_∞	Freestream wind speed (m/s)
C_T	Static torque coefficient, $c_T = T / (q_\infty R_r A_0)$	θ	Central angle of the overlapping blade arc or circular arc slot central angle (deg)
D	Wind turbine rotor diameter (m)	Θ	Rotor's angular position (deg)
bgr	Bucket gap width ratio	λ	Tip speed ratio, $\lambda = \omega R_r / V_\infty$
N	Number of buckets	μ_∞	Freestream air viscosity (Pa·s)
q_∞	Freestream dynamic pressure (Pa)	ρ_∞	Freestream air density (kg/m ³)
R_r	Wind turbine rotor radius (m)	φ	Slot's angular position (deg)
R	Wind turbine bucket radius (m)	Φ	Bucket arc (deg)
		ω	Angular velocity (rad/s)

1 Introduction

In recent years, numerical and experimental validations of 'S' type or Savonius rotor wind turbines have been added in the published literature. A series of studies conducted by different researchers have been presented, regarding the behaviour and the

performance output of Savonius wind turbines as it is expressed by the power and torque coefficients, in relation with the blade geometry. Savonius wind rotors with improved performance characteristics could lead to a rise of utilization of Savonius wind turbines as they have several advantages compared

with the horizontal axis wind turbines i.e. the simpler and the cheaper construction, better initial torque at lower wind speeds, lower noise levels, less wear on rotating parts, more rotor configuration options, smaller footprint occupation and the omnidirectional nature negating the need for a yawing mechanism [1]. Consequently, Savonius wind rotors could have a wider range of use and utilization in additional applications, particularly in the electricity needs of rural areas or covering partial loads in remote regions and the low cost decentralized power production [2]. Advanced blade configurations with improved performance characteristics, would be of much importance as they could extent the wind energy electricity generation by utilizing urban resources, where the present classic horizontal axis wind turbines would not be an appropriate selection since they are best performed in flat-terrain regions without obstacles [3]. A variety of models have been tested to determine the connection between the Savonius wind turbine performance and the different geometry design parameters. These configuration design parameters relate to the number of buckets, the rotor aspect ratio, the separation gap of rotor buckets, the profile change of the bucket cross-section, the overlap, the presence or absence of rotor endplates, the influence of bucket stacking and the presence of valves or gaps in the blades' midpoint, aiming to reduce the drag for the retreating blade [4-6].

Slotted bucket configurations of Savonius wind turbines have been sparsely explored by some researchers. Limited information is found in literature on exploring further the slot concept that Alaimo *et al.* [3, 7] presented in his work. A bucket configuration of the Savonius rotor was presented, implicating slots which have been examined with the Computational Fluid Dynamics (CFD) commercial software. Steady state CFD studies were performed aiming to explore the new configuration's behaviour regarding the starting torque and a parametrical analysis was conducted by changing the slot position on the bucket's running length. It was indicated that the placement of a slot in the bucket, towards the rotor's center, would improve the performance of the Savonius wind turbine only at lower tip speed ratios and would enhance the self-starting capability of the turbine. The slot's angle was investigated by testing different configurations with a constant slot position and a variable angle ranging only on the best performance configuration. There were no significant changes in the moment and the power coefficients, concluding that the slot angle is not a crucial factor in the overall turbine performance.

An implementation of a single slot was also attempted by Rahai [8] for optimizing a modified

blade for Savonius wind turbine. The slotted geometry design investigated, was not adopted since the introduced slot would not contribute to the overall improvement in the power performance. Rahai and Hefazi [8-9] introduced a complex blade shape that was finalized after an iteration process, using the NASA INS2D CFD software involving torque maximization algorithms with a modified version of the transfinite interpolation method. The slot placement was examined in the region where a flow separation was observed by the flow velocity-pressure contours at high angles of attack. The slot action was connected with the momentum injection to the other side of the blade, increasing the flow separation of the upper side for both upstream and downstream of the placed slot, thus, the amount of flow separation of the concave side was reduced, but the overall net effect of slot resulted in a loss of momentum, lower performances and a decrease of the efficiency.

In current research, the wind tunnel performance data of a two-bucket Savonius rotor [10] are compared with numerical results from slotted bucket rotors derived through the modification of the wind tunnel model bucket geometry. The solid buckets of the Savonius rotor model are replaced with slotted buckets consisting of partially overlapping blades that are placed in position, in order to utilize and take advantage of the lift forces applied on the blades, apart from the drag forces that a standard Savonius rotor relies for its rotation resulting to poor performance. Thus, the main objective of the current research is the CFD study of slotted bucket configurations of Savonius rotors and the prediction of their performance that are compared with the experimental data for the solid two bucket rotor [10]. The unsteady Reynolds-Averaged Navier-Stokes (RANS) equations are solved, using Fluent[®] [11] commercial code. A total of nine configurations of slotted bucket rotors are examined by introducing a geometry of a double slot bucket profile and the flow around the new wind turbine rotor is simulated to predict the performance output and the self-starting ability. Additionally, a parametrical study of geometry settings is included, aiming to investigate the central angle of the overlapping blade arc and the radial interspace between two overlapping blades.

2 Geometry aspects of the slotted bucket rotor

The conventional Savonius model rotor Config. No. 11, presented by Blackwell *et al.* [10] was used as the reference geometry for replacing the solid buckets with slotted. Each slotted bucket consists of three

partially overlapping circular arc blades forming two slots with the length and the width of the slots being the parameters of the configuration. Outline dimensions such as the rotor diameter and gap ratio, remain the same with the wind tunnel rotor Config. No. 11. A schematic view of Config. No. 11 rotor and a dimension summary is included in Fig. 1 (a) and Table 1 respectively.

Table 1 Geometry of Config. No. 11 Savonius rotor (Blackwell et al. 1978)

Description	Symbol	Value	Units
Number of buckets	N	2	-
Bucket arc	Φ	180	degress
Rotor's diameter	$D=4R-c$	950	mm
Bucket's radius	R	250	mm
Bucket gap width	c	50	mm
Bucket gap width ratio	$c/2R$	0.1	-

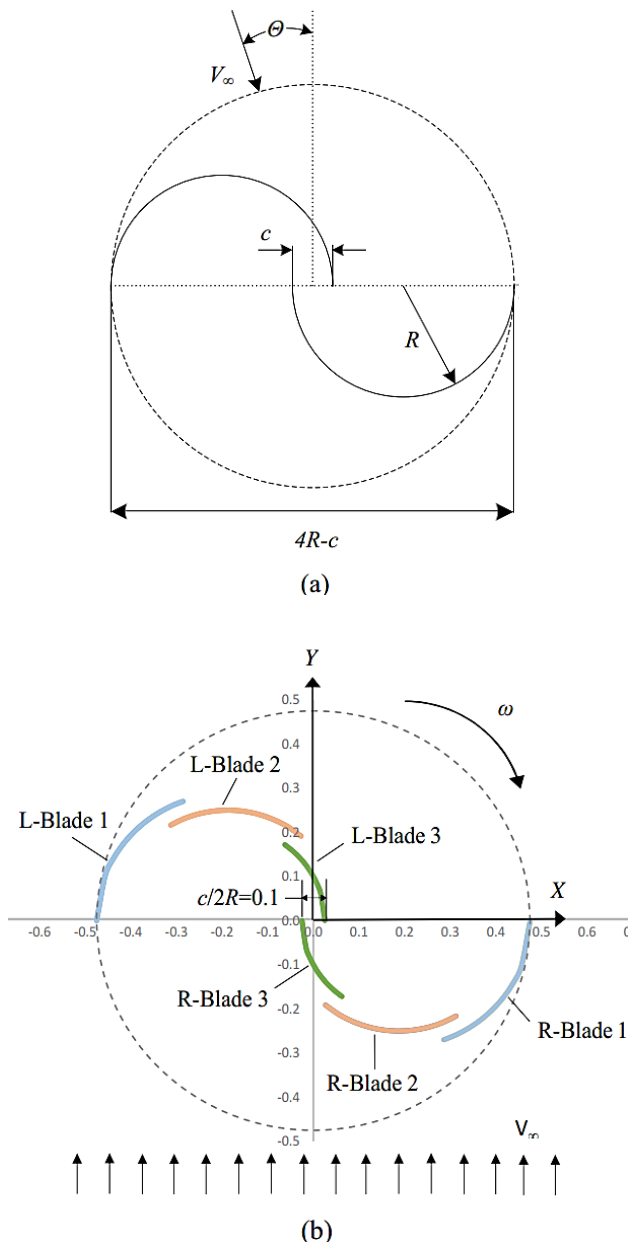


Fig. 1. Wind tunnel Savonius rotor - Configuration No. 11 (a) and the modified slotted bucket rotor (b).

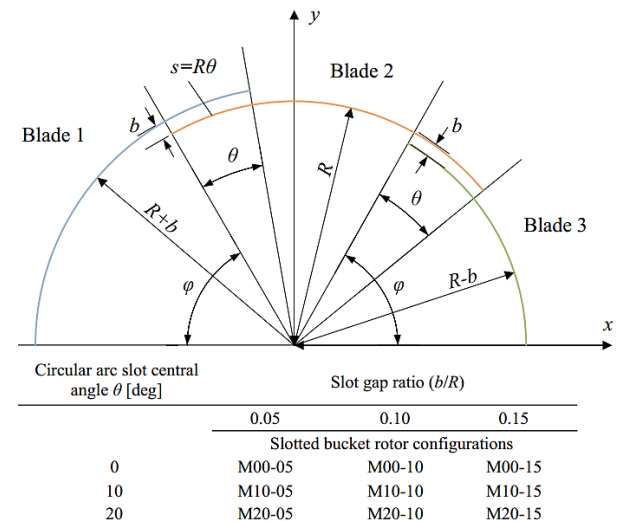


Fig. 2. Definition of the studied slotted bucket geometry and examined configurations.

Based on the reference rotor model, two slots between overlapping circular arc blades were placed at 60 deg and at 120 deg with the bucket coordinate system, (x,y) , located on bucket's arc center. The new bucket geometry contains three new subsections, named Blade 1, Blade 2, Blade 3 with the prefix "R" for the right bucket and "L" prefix for the left bucket. The center of each blade arc was maintained on the initial blade arc axis origin, but each end blade has different radius defined by the addition or subtraction of the slot width. In the present design, the slot length is also investigated since the circular arc slot central arc can be adjusted. The investigated slotted bucket rotor geometry is illustrated in Fig. 1 (b) and Fig. 2. The examined geometric parameters of the slotted-

bucket rotor models are the slot width ratio (b/R), expressing the dimensionless radial interspace between two overlapping blades and ranges from 0.05 to 0.15, and the central angle of the overlapping blade arc (θ) which defines the slot length ($s=R\theta$), ranges from 0 to 20 deg.

On the rotor bucket, each blade arc is described by a constrained circle equation. The equations used to export each blade in the (x,y) bucket coordinate system and the (X,Y) rotor coordinate system, are summarized as follows:

Left blade i ($i=1,2,3$):

$$X_{Li} = x_i - \left[(R - b) - \frac{c}{2} \right]; Y_{Li} = y_i \quad (1)$$

Right blade i ($i=1,2,3$):

$$X_{Ri} = -X_{Li}; Y_{Ri} = -Y_{Li} \quad (2)$$

Blade 1:

$$y_1 = \sqrt{(R + b)^2 - x_1^2}; x_1 \in [-(R + b), -(R + b)\cos(\varphi + \theta)] \quad (3)$$

Blade 2:

$$y_2 = \sqrt{R^2 - x_2^2}; x_2 \in [-R\cos\varphi, R\cos(\varphi - \theta)] \quad (4)$$

Blade 3:

$$y_3 = \sqrt{(R - b)^2 - x_3^2}; x_3 \in [R\cos\varphi, R - b] \quad (5)$$

where, $R=0.25$ m, $\varphi=60$ deg, $\theta=(0, 10$ and 20 deg), $b=(12.5, 25.0$ and 37.5 mm).

The radial interspace between two overlapping blades ratio or the slot width ratio, modified within the range of 5% and 15%, and the central angle of the overlapping blade arc or the circular arc slot central angle, modified within the range of 0 to 20 deg, are investigated for their influence on the power coefficient and the static torque. The previous parameters have been selected as variable inputs by

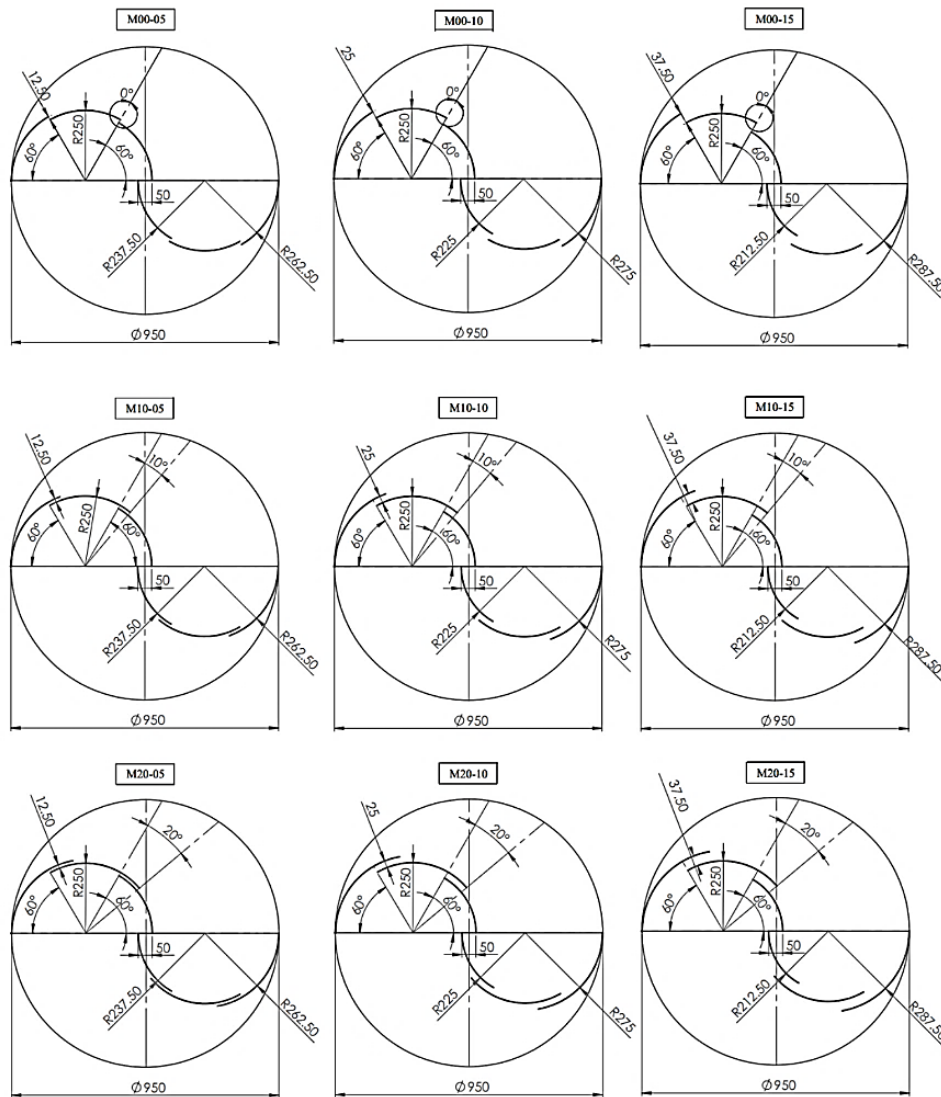


Fig. 3. Definition of the studied slotted bucket

maintaining constant the rest geometric parameters for producing the investigated slotted bucket rotor configurations. Nine selected configurations, representing each combination of the previous parameters, are presented in Fig. 2. The prefix M is used in the configuration code names, followed by the circular arc slot central angle value and the slot width ratio value. The schematic views of the selected configurations are illustrated with the finalized dimensions in Fig. 3.

3 Numerical calculations

3.1 Computational domain and boundary settings

The dimensions of the surrounding flow domain of the studied slotted bucket rotors are expressed in relation to the rotor's diameter (D). The origin of the rectangular shaped flow domain is located on the rotor's rotational axis and the length is extended by $6D$ upwind and $26D$ downstream in order to allow wake patterns to be fully deployed (Fig. 4). Sideways, the distance is $6D$ allowing the modelling of the generated vortices at rotor blade tips, which contribute to the induced drag. Symmetry was set on The constructed meshes have been designed aiming an acceptable mesh quality of the appropriate indices. The two-dimensional mesh, generated in Gambit® [12], consists of $3.25 \cdot 10^4$ elements with the 87% of the total cells concentrated in the rotor's rotating mesh region. An unstructured mesh was selected since it can be adapted better on complex curved shapes and the generation is more automated and faster than structured meshes. Grid independence was studied for the reference model, simulating further refined meshes that resulted in efficiency value change below 2%. The mesh was generated with quadrilateral elements with noticeable cells converted to paved quadrilaterals. Indices that were checked for the mesh quality are the aspect ratio, skewness and the orthogonal quality [13] that were shaped respectively to accepted values. Mesh adaption was performed on solver to reduce $\max y^+$ value below one, $y^+ \leq 1$ that is recommended for the selected turbulence model [14]. Mesh details for the reference non-modified model are shown in Fig. 5.

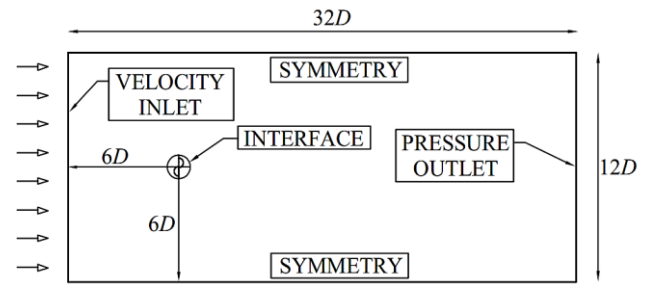


Fig. 4. Geometry of the computational domain.

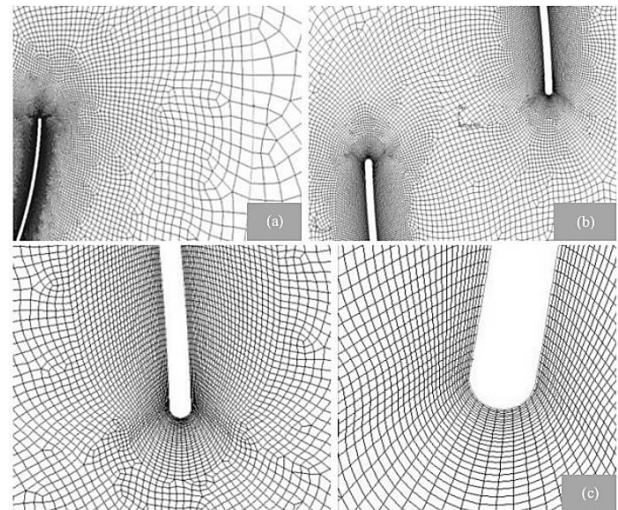
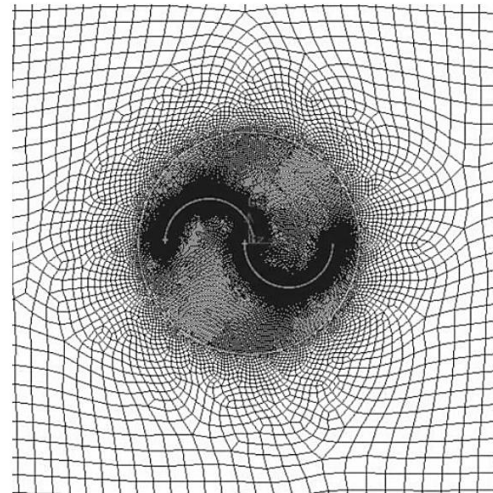


Fig. 5. Mesh overview for Savonius reference rotor and details (a) near the interface, (b) between the rotor gap, (c) at blade tip.

3.2 Simulations

For the current numerical modelling, two-dimensional viscous and incompressible flow was assumed in the computational domain. The unsteady Reynolds-Averaged Navier-Stokes (RANS)

equations were solved with Fluent's pressure-based solver using the Semi-Implicit Method for Pressure linked Equations (SIMPLE) algorithm for pressure-velocity coupling. A second order upwind scheme was used to discretize in finite-volume formulation the turbulent quantities and the flow variables. Sliding mesh model is used to solve the unsteady flow field. Spalart-Allmaras turbulence model was used, as numerous studies have used the specific model for Savonius rotor simulations, proving that can successfully predict the aerodynamic attributes of the wind turbine rotor [15-18]. The curved edges of the rotor blades were set as stationary walls with a no-slip condition, domain and rotor overlapping edges were set as contact interfaces, the surface domains were prescribed as fluid interiors and the rotor domain was set to moving mesh with different rotational velocities at a time, for achieving in each run the desirable tip speed ratio (λ) value. The air properties were set according to Sandia Laboratory's experimental data [10], i.e., 20 °C for the temperature, 1.204 kg/m³ for the density and 1.7894·10⁻⁵ Pa·s for the viscosity, resulting in Reynolds number per unit length (Re) 4.32·10⁵. A maximum number of iterations was set, along with the convergence criterion of six orders of magnitude residuals drop. For the steady state runs, a maximum of 3·10³ iterations with a drop of 10⁻⁵ of all scaled residuals was set, while for the transient flow runs, a maximum value of 50 iterations per time step was selected, before the solver jumps to the next time step with the same order of magnitude of the residuals drop.

4 Results and discussion

The numerical simulation performance results of wind tunnel two-bucket Savonius rotor Configuration No 11, $N=2$, $b_{gr}=0.1$ [10], are presented in Fig. 6. A good agreement of the selected Spalart-Allmaras turbulence model results can be noted up to tip speed ratio $\lambda=1.2$. Results for increased λ values are more overestimated, compared with lower λ values. A satisfying agreement with the experimental results is also noted for static torque (C_T), despite the overall slight overestimation in some regions. Weak validity spots are detected at the rotor's angular position of 75 and 125 deg, while the region of 0 to 55 deg is more overestimated. The final validation results have been accepted and the Spalart-Allmaras turbulence model was used to predict the performance and the flow characteristics for the slotted bucket-rotors at $Re=4.32\cdot 10^5$, for 7 m/s airflow velocity. The simulation results of the power coefficient (C_p) versus the tip speed ratio and the

static torque coefficient versus rotor's angular position curves of the different slotted-blade configurations, are presented in Fig. 7, Fig. 8 and Fig. 9. The results have been organized in groups according with the blade overlap range group.

The $C_p - \lambda$ curves indicate that all the examined slotted bucket rotors present a lower power performance than the reference solid bucket Savonius rotor. Among the configurations, the geometry named M00-05 that has a slot width ratio of 5% without blades overlapping, has the best power performance ($C_p=0.19$) in the range of $\lambda=0.8\sim 1$ for $Re=4.32\cdot 10^5$, which is about 20% lower than the standard Savonius rotor. Blades overlapping is not noticed to have a significant effect on the performance output, for the current geometries with fixed slot positions at 60 and 120 deg. The configuration groups of the same circular arc slot central angle and variable slot width ratio indicate a significant difference on the power coefficient for each λ solution set and that constitutes the slot width ratio an important design parameter for the power output performance of Savonius rotor modifications. Despite the reduced power performance, the static torque results indicate an improvement at low incidence angles compared with the Savonius rotor reference model. At the rotor's angular position of 0 to 55 deg and 145 to 165 deg for the most slotted bucket configurations, an increased average static torque value about 25% to 190% of the experimental value is observed. The best configuration (M00-05) has no negative static torque values and presents an average C_T value of 0.396 at 0 to 180 deg, which is improved compared to the solid bucket Savonius rotor that has an average C_T value of 0.303. The most inefficient configuration case is the M00-15 having 15% slot width ratio, which presented the lowest average $C_T=0.280$ with $C_T=-0.07$ at 55 deg rotor angular position, along with the M20-15 case, which had the lowest local $C_T=-0.188$ at 55 deg with an average $C_T=0.356$.

Next, the flow around the rotor was examined. Flow characteristics that relate to the performance output are addressed by visualizing the flow and examining the contours and the vectors of velocity around the bucket slots. The transient solution of the best and worst performed configurations (M00-05 and M20-15) are selected for further examination. Four selected frames of the last rotation corresponding to time steps which the rotor's

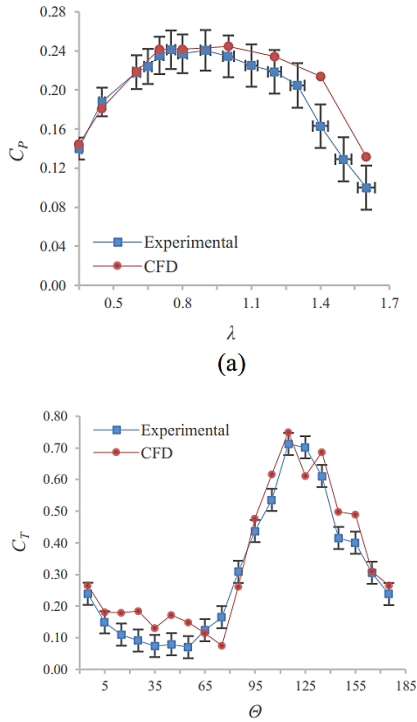


Fig. 6. Experimental and simulation results of power coefficient (a) and static torque coefficient (b) for Savonius wind tunnel rotor.

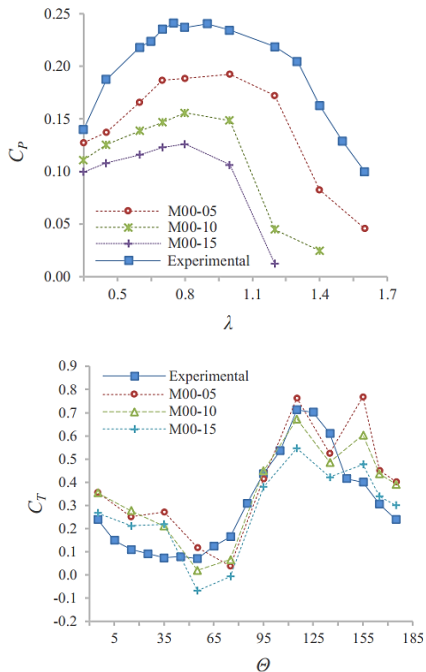


Fig. 7. Computed power coefficient versus tip speed ratio and static torque coefficient versus rotor angle for the M00-xx group of the studied slotted bucket rotors, compared with the corresponding measurements of solid bucket Savonius rotor.

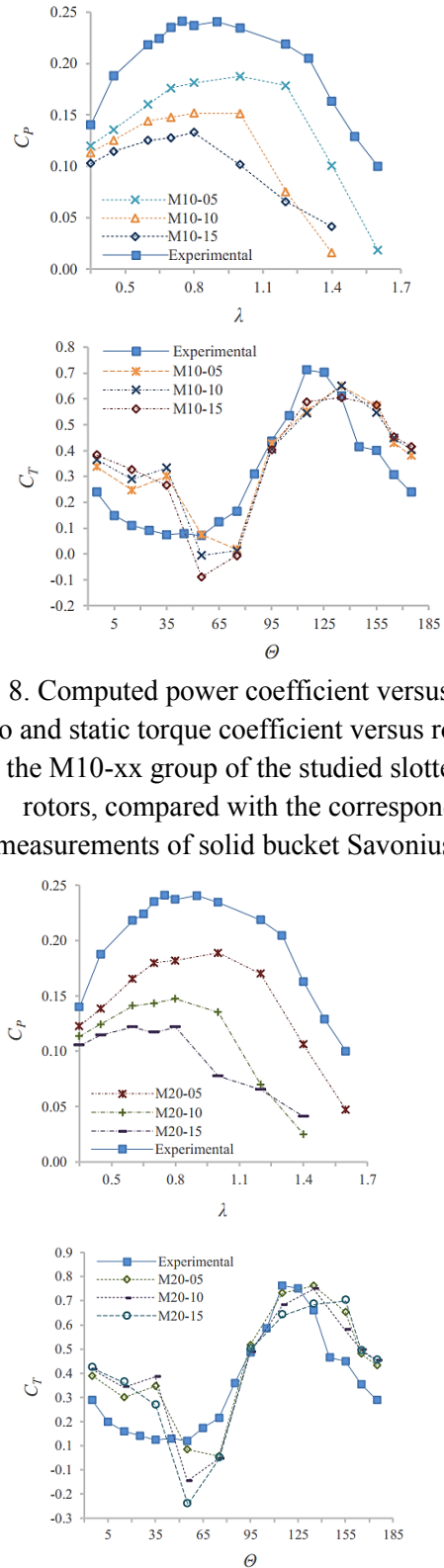


Fig. 8. Computed power coefficient versus tip speed ratio and static torque coefficient versus rotor angle for the M10-xx group of the studied slotted bucket rotors, compared with the corresponding measurements of solid bucket Savonius rotor.

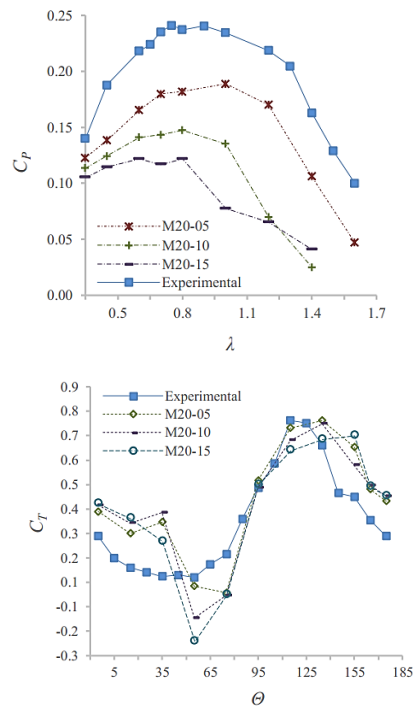


Fig. 9. Computed power coefficient versus tip speed ratio and static torque coefficient versus rotor angle for the M20-xx group of the studied slotted bucket rotors, compared with the corresponding measurements of solid bucket Savonius rotor.

angular position is 0, 45, 90 and 135 degrees, are included in Fig. 10 to Fig. 13, for $\lambda=0.8$. The interval of 45 degrees is selected in order to represent equally a semi cycle rotor rotation, along with the 0 deg angle for which the air incidents perpendicularly the convex and the concave side of the advancing and

returning blade. At 0 deg angle, the same flow structure characteristics with the reference Savonius rotor are observed in terms of the acceleration at the tip of the advancing blade and the stagnation point on the concave side of the returning blade. More boundary layer separation regions are noted on the

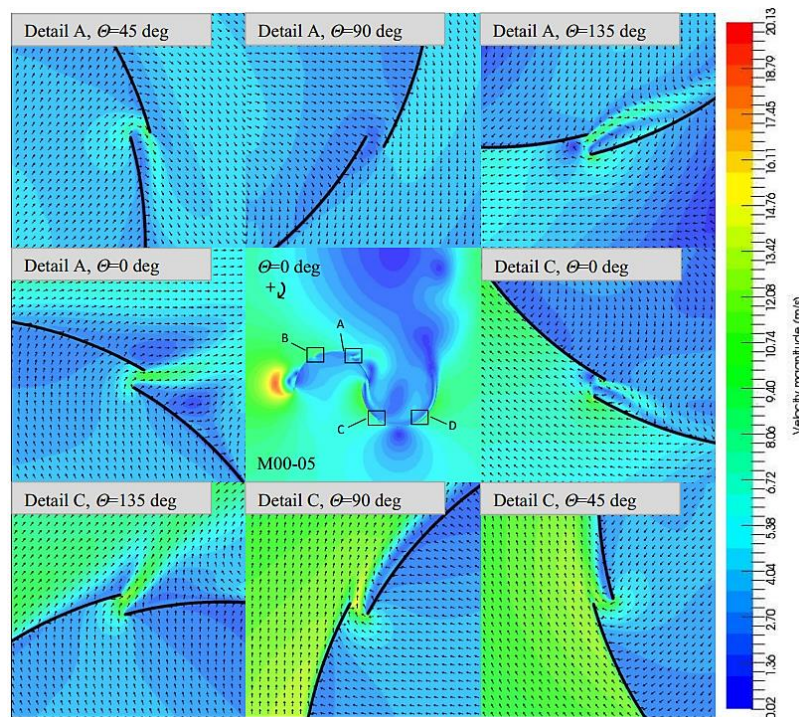


Fig. 10. Flow through bucket slots A and C at 0, 45, 90 and 135 degrees rotor position, for M00-05 configuration at $\lambda=0.8$.

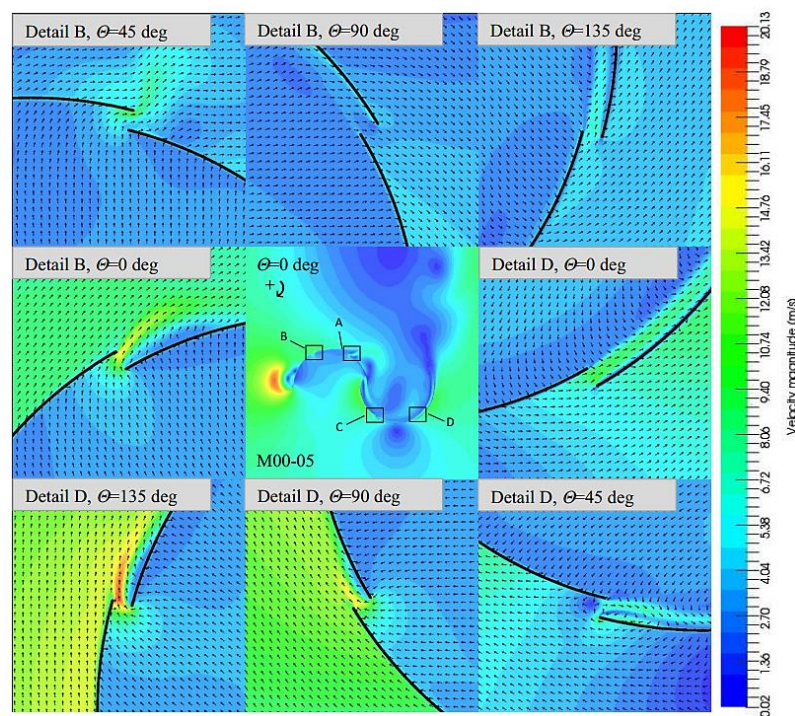


Fig. 11. Flow through bucket slots B and D at 0, 45, 90 and 135 degrees rotor position, for M00-05 configuration at $\lambda=0.8$.

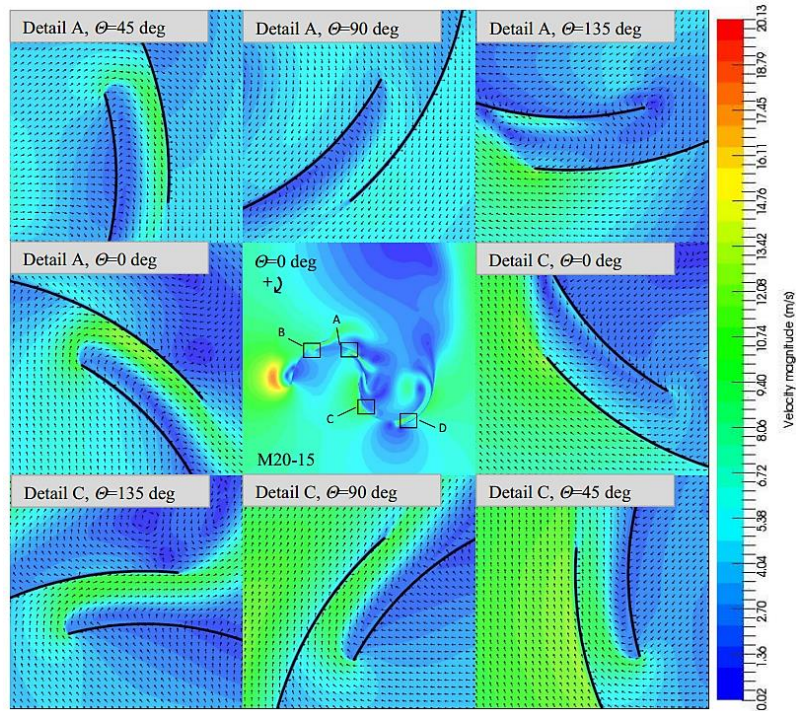


Fig. 12. Flow through bucket slots A and C at 0, 45, 90 and 135 degrees rotor position, for M20-15 configuration at $\lambda=0.8$.

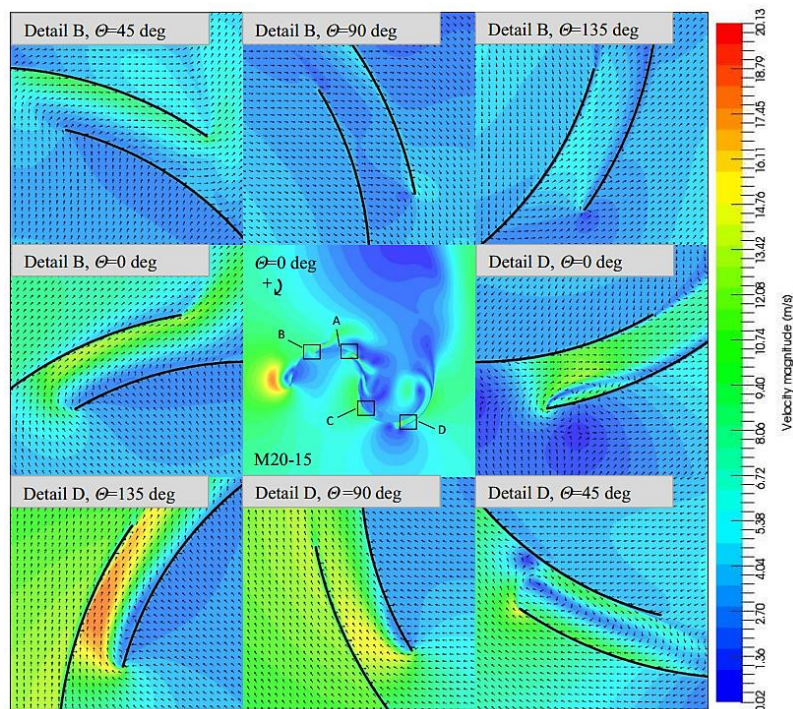


Fig. 13. Flow through bucket slots B and D at 0, 45, 90 and 135 degrees rotor position, for M00-05 configuration at $\lambda=0.8$.

walls of the sub-blades of advancing rotor blade. At the 45 deg angle where the Savonius rotor presents low C_T value, the recirculation of flow behind the advancing blade gets more intense. The stagnation zone is displaced on the second slot on the returning blade where flow is observed to pass to the concave

side of the returning blade, reducing the opposing torque applied on rotor. This improvement is reduced by the same event occurring on the advancing blade where the flow pass from concave to convex side. At the 135 deg rotor angle where the Savonius presents a high static torque value, the flow is noted to

accelerate towards the wind flow direction on the convex side of the advancing blade, which is the lift generation mechanism driving the rotor, apart from the drag forces exerted on concave side of advancing blade. The introduced gap between the first and the second blade amplify this effect by inserting more airflow from the concave side to the convex side. The slots on the returning blade that allow the air to pass through the blade, are also beneficial for the current angle and the overall torque balance. However, more stagnation points appear near the increased slot width space of M20-15 and additional recirculation areas are observed locally between the gaps, contributing to the decreased power output performance.

5 Conclusion

It was concluded that all the examined slotted bucket configurations present a lower average power coefficient compared with the conventional model of Savonius rotor. However, the static investigation of the slotted bucket configurations, revealed improved static torque coefficients in the configurations with reduced slot width ratio values. Implementing double slots in fixed positions resulted in a new way for modifying the classical Savonius bucket rotor, with a trade-off between achieving better self-starting characteristics and reducing slightly the turbine's efficiency. Two of the most important parameters associated with the slot implementation which are the slot width ratio and the circular arc slot central angle, have been examined aiming to investigate their effect on the performance attributes. The slot width ratio was noticed to have greater influence on the power output performance, since low values relate to improved efficiency, while increased values of slot width ratio lead to reduced power coefficients. The second examined parameter of the circular arc slot central angle had the least influence, since no significant changes were observed at the output performance characteristics.

The flow structure flow around the rotor had an increased level of complexity. The implementation of slots complicates further the flow around the rotor, since more flow separation points can be observed, and additional vortices appear behind the rotor and near the slots. Additional stagnation points and flow separation regions with flow recirculation, are spotted in regions where are not reported on classic Savonius rotors. The previous observation combined with the unwanted flow passing from concave to convex side of the advancing blade, are assumed to be the main causes of inferior power performance.

References:

- [1] B. D. Altan and M. Atilgan, "A study on increasing the performance of Savonius wind rotors," *Journal of mechanical science and technology*, vol. 26, no. 5, pp. 1493–1499, 2012. <https://doi.org/10.1007/s12206-012-0313-y>
- [2] J. Abraham, B. Plourde, G. Mowry, W. Minkowycz, and E. Sparrow, "Summary of Savonius wind turbine development and future applications for small-scale power generation," *Journal of Renewable and Sustainable Energy*, vol. 4, no. 4, p. 042703, 2012. <https://doi.org/10.1063/1.4747822>
- [3] A. Alaimo, A. Esposito, A. Milazzo, C. Orlando, and F. Trentacosti, "Slotted blades savonius wind turbine analysis by CFD," *Energies*, vol. 6, no. 12, pp. 6335–6351, 2013. <https://doi.org/10.3390/en6126335>
- [4] J. V. Akwa, H. A. Vielmo, and A. P. Petry, "A review on the performance of Savonius wind turbines," *Renewable and Sustainable Energy Reviews*, vol. 16, no. 5, pp. 3054–3064, 2012. <https://doi.org/10.1016/j.rser.2012.02.056>
- [5] M. M. A. Bhutta, N. Hayat, A. U. Farooq, Z. Ali, S. R. Jamil, and Z. Hussain, "Vertical axis wind turbine—A review of various configurations and design techniques," *Renewable and Sustainable Energy Reviews*, vol. 16, no. 4, pp. 1926–1939, 2012. <https://doi.org/10.1016/j.rser.2011.12.004>
- [6] S. Roy and U. K. Saha, "Review on the numerical investigations into the design and development of Savonius wind rotors," *Renewable and Sustainable Energy Reviews*, vol. 24, pp. 73–83, 2013. <https://doi.org/10.1016/j.rser.2013.03.060>
- [7] A. Alaimo, A. Milazzo, F. Trentacosti, and A. Esposito, "On the Effect of Slotted Blades on Savonius Wind Generator Performances by CFD Analysis," in *Advanced Materials Research*, 2012, vol. 512, pp. 747–753. <https://doi.org/10.4028/www.scientific.net/AMR.512-515.747>
- [8] H. R. Rahai and H. Hefazi, "Vertical axis wind turbine with optimized blade profile," *US7393177 B2*, 01-Jul-2008.
- [9] H. R. Rahai and H. Hefazi, "Development of optimum design configuration and performance for vertical axis wind turbine: Feasibility Analysis and Final EISG Report," *California Energy Commission Publications*, CEC-500-2005-084, 2005.
- [10] B. F. Blackwell, R. F. Sheldahl, and L. V. Feltz, *Wind tunnel performance data for two- and three-bucket Savonius rotors*. Sandia

Laboratories, Albuquerque, N.M. (USA), SAND76-0131, 1977.

- [11] Fluent Inc., “FLUENT 6.3.26 User’s Guide.” 2006.
- [12] Fluent Inc., “GAMBIT 2.4.6 User’s Guide.” 2006.
- [13] A. Katz and V. Sankaran, “High aspect ratio grid effects on the accuracy of Navier–Stokes solutions on unstructured meshes,” *Computers & Fluids*, vol. 65, pp. 66–79, 2012. <https://doi.org/10.1016/j.compfluid.2012.02.012>
- [14] Pr. Spalart and S. Allmaras, “A one-equation turbulence model for aerodynamic flows,” in 30th Aerospace sciences meeting and exhibit, 1992, p. 439. <https://doi.org/10.2514/6.1992-439>
- [15] K. Rogowski and R. Maroński, “CFD computation of the Savonius rotor,” *Journal of Theoretical and Applied Mechanics*, vol. 53, no. 1, pp. 37–45, 2015. <http://dx.doi.org/10.15632/Jtam-pl.53.1.37>
- [16] S. Xiaojing, C. Yajun, W. Guoqing, and H. Diangui, “Research on the aerodynamic characteristics of a hybrid lift/drag-based vertical axis wind turbine,” presented at the 9th Annual Green Energy Conference, Tianjin China, 2014. <https://doi.org/10.1177/2F1687814016629349>
- [17] Y. Lee, “Wind turbine simulation for time - dependent angular velocity, torque and power,” *International Journal of Engineering Science and Technology*, vol. 1, no. 5, pp. 321–328, 2013.
- [18] J. Świryczuk, P. Doerffer, and M. Szymaniak, “Unsteady flow through the gap of Savonius turbine rotor,” *Task Quarterly*, vol. 15, no. 1, pp. 59–70, 2011.

Creative Commons Attribution License 4.0 (Attribution 4.0 International, CC BY 4.0)

This article is published under the terms of the Creative Commons Attribution License 4.0

https://creativecommons.org/licenses/by/4.0/deed.en_US

Contribution of individual authors to the creation of a scientific article

Chasiotis Vasileios carried out the simulation, analysis, data curation, visualisation and writing the original draft, Tachos Nikolaos carried out the methodology and simulation and Filios Andronikos was responsible for the overall supervision.

Sources of funding for research presented in a scientific article or scientific article itself

The authors declare that there is no conflict of interest in this paper. No financial support was received to carry out this study.